International Journal of Mathematical Applications and Solutions
Vol 1, Issue 1 2025

# Unstable MHD Flow with Soret-Dufour and Second-order Chemical Reaction Past a Vertical Porous Plate at Variable Suction Velocity

**Khurram Iqbal[1], Fawad Alam[2]**
**Department of Actuarial Sciences, Mathematics and Statistics, Institute of Business Management, Karachi, Pakistan.**

**Mathlogix publications**

***Article Info***

***Received: 30-05-2025 Revised:08-06-2025 Accepted:19-06-2025 Published:29-06-2025***

**Abstract:** This work aims to investigate the combined effects of radiation, Soret-Dufour, and second order chemical reactions on unsteady magnetohydrodynamic (MHD) flow across a vertical porous plate submerged in a porous medium under varying suction velocity. The Crank-Nicolson implicit finite difference approach has been used to numerically solve the nonlinear partial differential equation of the flow issue in this model. The features of skin friction, Nusselt number, and Sherwood number are presented with the aid of the table, while the parameters of velocity, temperature, and concentration are shown visually.

**MSC:** 76W05, 80A20, 80A21, 80A32, 80M20.

**Keywords:** Magnetohydrodynamics, Heat Transfer, Mass Transfer, Order of chemical reaction, Soret and Dufour effects, Crank- Nicolson finite difference method.

## 1. Introduction

Natural convection MHD flow of second-order chemical reactions with Soret Dufour and radiation effects is used in a variety of chemical industries, including drying, food processing, oil extraction, and solid mechanics. This is the reason why a lot of researchers are drawn to this study. Radiative-convective flow is also widely used in astrophysical fluxes and thermal chambers for heating and cooling. The burning pool of oil, leaching by spray, and drying all illustrate the fluid dynamics theory of mass transfer. Because of their uses in engineering and the sciences, such as isotope separation, several researchers looked into how Soret and Dufour affected the flow difficulties.

The numerical result of nonlinear radiation for heat transport of nanofluid across a vertical plate was examined by Sandeep and Babu [1]. Unsteady nanofluid flow phenomena in the presence of higher order chemicals were studied by Rushi et al. [2]. The MHD boundary layer slip flow and heat transfer of a power-law fluid across a flat plate were studied by Mastroberardino et al. [3]. Change SoretDufour on MHD flow of viscoelastic fluid across a semi-infinite vertical plate is examined by Idowu and Falodun [4]. The combined effects of Soret and Dufour on the MHD flow of a power-law fluid across a flat plate in a slip flow regime were investigated by Saritha et al. [5]. The effects of second-order chemical reactions on MHD free convection dissipative fluid flow via an inclined porous surface through heat generation were examined by Malik and Rahman [6].

The effects of Soret and Dufour on the flow of a viscous fluid via a curved stretching surface were noted by Imtiaz et al. [7]. Soret and Dufour effects on MHD mixed convection flow approaching a vertical plate in a porous media were investigated by Anuradha and Harianand [8]. The precise solution of heat and mass

transport in MHD Poiseuille flow with porous walls was investigated by Ahmed [10]. In the presence of a heat source and a chemical reaction, Das and Dorjee [11] examined the MHD flow using the Soret and Dufour effects. The current study examines how radiation, second-order chemical reactions, and Soret-Dufour affect the unsteady MHD flow of a viscous incompressible fluid through a vertical porous plate submerged in a porous medium while taking changing suction velocity into account. By using the Crank-Nicolson implicit finite difference method to solve the governing equations of the flow field while taking changes with suitable parameters into account, the result of variations in various parameters on velocity, heat transfer, and mass transfer as well as in physical quantities like skin friction, Nusselt number, and Sherwood number is obtained.

## 2. Formulation of Model

In this model, we consider a fluid capable of a second-order chemical reaction and an unsteady MHD boundary layer flow of a viscous incompressible electrically conducting fluid past a semi-infinite vertical porous plate immersed in a porous medium. Our assumption in starting the plate moves with velocity $u_0$ and concentration and temperature decrease exponentially

with respect to time and the plate gets heated at temperature $\breve{\Theta}_w$ and concentration $\breve{\Phi}_w$. The $x\breve{}$-axis considered along with the semi-infinite plate in the vertically upward direction and $y\breve{}$-axis normal to it, the flow variables are functions of normal distance $y\breve{}$ and $t\breve{}$ only. A magnetic field $B_0$ is exerted normal to the plate, the induced magnetic field is neglected because of under low magnetic Reynolds number. Suction velocity is considered time-dependent and normal to the plate. We further consider that the plate is non-conducting. From the above model of the problem, the governing equations of flow field under the usual Boussinesq approximation are as follows:

Equation of Continuity:

$$\frac{\partial v\breve{}}{\partial y\breve{}} = 0 \tag{1}$$

Equation of momentum:

$$\frac{\partial \breve{u}}{\partial t\breve{}} + v\breve{}\frac{\partial \breve{u}}{\partial y\breve{}} = \nu\frac{\partial \breve{u}}{\partial y\breve{}^2} + g\beta_t(\breve{\Theta} - \breve{\Theta}_\infty) + g\beta_c(\breve{\Phi} - \breve{\Phi}_\infty) - \frac{\sigma B_0^2 \breve{u}}{\rho} - \frac{\nu \breve{u}}{\breve{K}} \tag{2}$$

Energy Equation:

$$\rho c_p \left(\frac{\partial \breve{\Theta}}{\partial t\breve{}} + v\breve{}\frac{\partial \breve{\Theta}}{\partial y\breve{}}\right) = k\frac{\partial^2 \breve{\Theta}}{\partial y\breve{}^2} - \frac{\partial q_r}{\partial y\breve{}} + \frac{\rho D_m k_\Theta}{c_s}\frac{\partial^2 \breve{\Phi}}{\partial y\breve{}^2} \tag{3}$$

Equation of mass transfer:

$$\frac{\partial \breve{\Phi}}{\partial t\breve{}} + v\breve{}\frac{\partial \breve{\Phi}}{\partial y\breve{}} = D_m\frac{\partial^2 \breve{\Phi}}{\partial y\breve{}^2} + \frac{D_m k_\Theta}{\Theta_m}\frac{\partial^2 \breve{\Theta}}{\partial y\breve{}^2} - k_r(\breve{\Phi} - \breve{\Phi}_\infty) \tag{4}$$

The initial and boundary conditions for this model are

$$\begin{aligned} &t\breve{} \le 0 \quad u\breve{} = 0 \quad \breve{\Theta} = \breve{\Theta}_\infty \quad \breve{\Phi} = \breve{\Phi}_\infty \quad \forall\, y\breve{} \\ &t\breve{} > 0 \qquad u\breve{} = u_0 \quad \breve{\Theta} = \breve{\Theta}_\infty + g(\breve{\Theta}_w - \breve{\Theta}_\infty)e^{-n\breve{t}}, \\ &\breve{\Phi} = \breve{\Phi}_\infty \qquad + g(\breve{\Phi}_w - \breve{\Phi}_\infty)e^{-n\breve{t}}, \quad at\, y\breve{} = 0 \\ &u\breve{} = 0 \qquad \breve{\Theta} \to \breve{\Theta}_\infty \quad \breve{\Phi} \to \breve{\Phi}_\infty \quad y\breve{} \to \infty \end{aligned} \tag{5}$$

where $\breve{\Theta}$ and $\breve{\Phi}$ are temperature and concentration , $\breve{\Phi}_\infty$ and $\breve{\Theta}_\infty$ are concentration and temperature of free stream boundary layer, $k_r$ is chemical reaction parameter constant, $\beta_t$ is coefficient of volumetric thermal expansion of the fluid, $\beta_c$ is volumetric coefficient of expansion with concentration of fluid, $q_r$ is radiative heat along $y\breve{}$-axis, $\nu$ is kinematic viscosity and $\Theta_m$ is mean fluid temperature, $\breve{K}$ is permeability of porous medium, $\sigma$ is electrical conductivity, $D_m$ is molecular diffusivity, $g$ is acceleration due to gravity, $K_\Theta$ is thermal diffusion ratio, $\mu$ is viscosity, $\rho$ is fluid density, $k$ is thermal conductivity of fluid, $c_p$ is specific heat at constant pressure.

Integrating both sides of the continuity equation (1), we get $v\breve{} =$ constant. It is obvious that the suction velocity normal to the plate is a constant function or consider as a function of time. In this model, we assume as a case when it is both

constant and time-dependent and expressed as

$$v\breve{} = -u_0(1 + gAe^{n\breve{t}}) \tag{6}$$

where $u_0$ is mean suction velocity, which is a non-zero positive constant and the minus sign indicates that the suction is outwards the plate. $A$ is the suction parameter, $g$ is a small reference parameter and $gA \ll 1$. The radiative flux term $q_r$ by using the Rosseland approximation [12], is given by

$$q_r = -\frac{4\tilde{\sigma}}{3a_r}\frac{\partial \breve{\Theta}^4}{\partial y\breve{}} \tag{7}$$

where $a_r$ is Rosseland radiation absorptivity constant and $\tilde{\sigma}$ is Stefan Boltzmann constant. In this problem, $\breve{\Theta}^4$ can be expressed as linearly with temperature because the temperature difference within a flow is very small. It is seen by

expanding in Taylor's series about $\breve{\Theta}_\infty$ and considering the negligible higher-order term, so

$$\breve{\Theta}^4_\infty \cong 4\breve{\Theta}^3_\infty \breve{\Theta} - 3\breve{\Theta}^4_\infty \tag{8}$$

so, with the help of equations (7) and (8), equation (3) is reduced to

$$\rho c_p\left(\frac{\partial \breve{\Theta}}{\partial \breve{t}} + v\breve{}\frac{\partial \breve{\Theta}}{\partial y\breve{}}\right) = k\frac{\partial^2 \breve{\Theta}}{\partial y\breve{}^2} + \frac{16\sigma\breve{\Theta}^3_\infty}{3k_m}\frac{\partial^2 \breve{\Theta}}{\partial y\breve{}^2} + \frac{\rho D_m k_\Theta}{c_s}\frac{\partial^2 \breve{\Phi}}{\partial y\breve{}^2} \tag{9}$$

In continuation of getting the non-dimensional form of governing partial differential equations, we introduce the following non-dimensional quantities

$$\begin{aligned} n &= \frac{\nu \breve{n}}{u_0^2}, \quad u = \frac{u\breve{}}{u_0}, \quad t = \frac{\breve{t}u_0^2}{\nu}, \quad \theta = \frac{\breve{\Theta} - \breve{\Theta}_\infty}{\breve{\Theta}_w - \breve{\Theta}_\infty}, \quad C = \frac{\breve{\Phi} - \breve{\Phi}_\infty}{\breve{\Phi}_w - \breve{\Phi}_\infty}, \quad Gm = \frac{\nu g\beta_c(\breve{\Phi}_w - \breve{\Phi}_\infty)}{u_0^3}, \\ Gr &= \frac{\nu g\beta_t(\breve{\Theta}_w - \breve{\Theta}_\infty)}{u_0^3}, \quad y = \frac{y\breve{}u_0}{\nu}, \quad K_r = \frac{k_r\nu}{u_0^2}, \quad Du = \frac{D_m k_\Theta(\breve{\Phi}_w - \breve{\Phi}_\infty)}{c_s c_p \nu(\breve{\Theta}_w - \breve{\Theta}_\infty)}, \quad M = \frac{\sigma B_0^2}{\rho u_0^2}, \\ So &= \frac{D_m k_\Theta(\breve{\Theta}_w - \breve{\Theta}_\infty)}{\Theta_m \nu(\breve{\Phi}_w - \breve{\Phi}_{hi\infty})}, \quad R = \frac{4\tilde{\sigma}\breve{\Theta}^3_\infty}{a_r k}, \quad Sc = \frac{\nu}{D_m}, \quad K = \frac{u_0^2 \breve{K}}{\nu^2}, \quad Pr = \frac{\mu c_p}{k}. \end{aligned} \tag{10}$$

Here $Gm$, $Gr$, $Kr$, $Du$, $M$ , $So$, $R$, $Sc$, $K$ and $Pr$ are respectively free convection parameter due to concentration, free convection parameter due to temperature, rate of chemical reaction parameter, Dufour number, magnetic parameter, Soret number, radiation parameter, Schmidt number, Darcy permeability parameter, and Prandtl number. Employing above dimensionless variables in equations (2), (9) and (4), we get non dimensional form of non linear partial differential equations:

$$\frac{\partial u}{\partial t} - (1 + gAe^{nt})\frac{\partial u}{\partial y} = \frac{\partial^2 u}{\partial y^2} + Gr\,\theta + Gm\,C - M\,u + \frac{u}{K} \tag{11}$$

$$\frac{\partial \theta}{\partial t} - \left(1 + gAe^{nt}\right)\frac{\partial \theta}{\partial y} = \frac{1}{Pr}\left(1 + \frac{4}{3}R\right)\frac{\partial^2 \theta}{\partial y^2} + Du\frac{\partial^2 C}{\partial y^2}$$

$$\frac{\partial C}{\partial t} - \left(1 + gAe^{nt}\right)\frac{\partial C}{\partial y} = \frac{1}{Sc}\frac{\partial^2 C}{\partial y^2} + Sr\frac{\partial^2 \theta}{\partial y^2} - K_r C^2 \tag{13}$$

with the initial and boundary conditions:

$$\begin{aligned} &\text{for } t \le 0 \quad u = 0, \quad \theta = 0, \quad C = 0, \quad \forall\, y \\ &\text{for } t > 0 \quad u = 1, \quad \theta = 1 + ge^{-nt}, \quad C = 1 + ge^{-nt}, \quad at\ y = 0 \\ &u = 0, \quad \theta \to 0, \quad C \to 0, \quad y \to \infty. \end{aligned} \tag{14}$$

Mathematical expression for physical parameters skin-friction, Nusselt number and Sherwood number for primary interest of this type boundary layer flow problem are

$$\tau = \left(\frac{\partial u}{\partial y}\right)_{y=0}$$

$$Nu = -\left(\frac{\partial \theta}{\partial y}\right)_{y=0} \tag{15}$$

$$Sh = -\left(\frac{\partial C}{\partial y}\right)_{y=0}$$

## 3. Procedure of Solution

Equations (11), (12) and (13) represent non dimensional form of velocity, heat transfer and mass transfer equations, equation (14) represents non dimensional form of boundary conditions and these equations and boundary conditions are non linear partial differential equations. So the exact solution of this type of system of partial differential equations is not possible. Crank-Nicolson implicit finite difference method is used to get a numerical solution. Converted form of these systems of partial differential equations after employing Crank-Nicolson finite difference are:

$$\frac{u_{i,j+1} - u_{i,j}}{\Delta t} - \left(1 + gAe^{nj\Delta t}\right)\frac{u_{i+1,j} - u_{i,j}}{\Delta y} = \frac{\left(u_{i-1,j} - 2u_{i,j} + u_{i-1,j} - 2u_{i,j+1} + u_{i+1,j+1}\right)}{2(\Delta y)^2} + Gr\left(\frac{\theta_{i,j+1} - \theta_{i,j}}{2}\right) + Gm\left(\frac{C_{i,j+1} - C_{i,j}}{2}\right) - \left(M + \frac{1}{K}\right)\left(\frac{u_{i,j+1} + u_{i,j}}{2}\right) \tag{16}$$

$$\frac{\theta_{i,j+1} - \theta_{i,j}}{\Delta t} - \left(1 + gAe^{nj\Delta t}\right)\frac{\theta_{i+1,j} - \theta_{i,j}}{\Delta y} = \frac{1}{Pr}\left(1 + \frac{4R}{3}\right)\frac{\left(\theta_{i-1,j} - 2\theta_{i,j} + \theta_{i-1,j} - 2\theta_{i,j+1} + \theta_{i+1,j+1}\right)}{2(\Delta y)^2} + Du\left(C_{i-1,j} - 2C_{i,j} + C_{i-1,j} - 2C_{i,j+1} + C_{i+1,j+1}\right), \tag{17}$$

$$\frac{C_{i,j+1} - C_{i,j}}{\Delta t} - \left(1 + gAe^{nj\Delta t}\right)\frac{C_{i+1,j} - C_{i,j}}{\Delta y} = \frac{1}{Sc}\left(\frac{C_{i-1,j} - 2C_{i,j} + C_{i-1,j} - 2C_{i,j+1} + C_{i+1,j+1}}{2(\Delta y)^2}\right) + So\left(\frac{\theta_{i-1,j} - 2\theta_{i,j} + \theta_{i-1,j} - 2\theta_{i,j+1} + \theta_{i+1,j+1}}{2}\right), - K_r\left(\frac{C_{i,j+1} + C_{i,j}}{2}\right)^2 \tag{18}$$

initial and boundary conditions are also written as:

$$\begin{aligned} &u_{i,0} = 0 \quad \theta_{i,0} = 0 \quad C_{i,0} = 0 \quad \forall\, i \\ &u_{0,j} = 1 \quad \theta_{0,j} = 1 + ge^{-nj\Delta t} \quad C_{0,j} = 1 + ge^{-nj\Delta t} \\ &u_{N,j} = 0 \quad \theta_{N,j} \to 0 \quad C_{N,j} \to 0 \end{aligned} \tag{19}$$

where node $i$ represents partition of $y$, $\Delta y = y_{i+1} - y_i$ and node $j$ represents to partition of time $t$, $\Delta t = t_{j+1} - t_j$ .Calculating values of $u$, $\theta$ and $C$ at time $t$.

We compute the values at time $t + \Delta t$ as following method: we substitute $i = 1, 2, ..., N-1$, where $N$ indicate to $\infty$, equations (16) to (18) give tridiagonal system of equations with initial and boundary conditions in equation (19), are solved by using Thomos algorithm as given in Carnahan et al. [9], we find the values of $\theta$ and $C$ for all $y$ at $t + \Delta t$. Equation (16) is solved by same method to replace these values of $\theta$ and $C$, we find solution of $u$ till required time $t$.

## 4. Results and Discussion

In continuation of discussion physical behavior of the problem, the numerical analysis of velocity, temperature, concentration, Skin-friction coefficient, Nusselt number and Sherwood number over the boundary layer for different values of flow parameters like magnetic parameter $M$, rate of chemical reaction parameter $K_r$, radiation parameter $R$, Soret number $So$, Prandtl number $Pr$, Schmidt number $Sc$, Dufour number $Du$ and time t. In our investigation the values of thermal Grashof number $Gr$, solutal Grashof number $Gm$, Darcy permeability parameter $K$, small reference parameter $g$, suction parameter $A$ and constant $n$ were fixed as 4, 6, 1.5, 0.02, 0.2 and 4 respectively.

With an increase in $Du$ in figure 13, it is seen that velocity profiles increase slowly between the plate and boundary layer and it is also analyzed that at some distance from plate, velocity maintains constant after then goes to zero at the boundary layer. Temperature profiles increase in figure 14 as $Du$ increases. Figure 15 depicts that concentration profiles decrease slowly near to plate on increasing $Du$. Figure 1 shows velocity profiles decreases in figure 1 and temperature profiles in figure 3 slightly increases near to plate while concentration profiles in figure 2 decreases rapidly near to plate as $Kr$ increases.

Figure 10 drawn for various values of $Pr$ on velocity profiles. It is seen that velocity profiles decrease rapidly near to boundary layer as $Pr$ increases. Temperature profiles in figure 11 decreases as $Pr$ increases. It is a good symptom with physical behavior that an increase in $Pr$ leads to a decrease in thickness of the temperature boundary layer. Concentration profiles in figure 12 near to wall increases after then decreases when $Pr$ increases. Higher Soret number $So$ increases fluid velocity profiles in figure 17, decreases fluid temperature near to plate in figure 18 and increases concentration profiles in figure 19. Figure 16 shows that an increase in $M$ leads to increases in velocity profiles of fluid. Velocity profiles increases in figure 7 as $R$ increases, because of the increase in radiation parameter releases thermal energy to flow. It is obvious that on increase $R$, temperature profiles in figure 8 increases while concentration profiles in figure 9 decreases. Figure 4 shows the effect of $Sc$ on velocity profiles. It is seen that on increase $Sc$, velocity profiles decrease rapidly after then decreases slowly. Temperature profiles increase slowly near to plate in figure 5 when $Sc$ increases. Concentration profiles in figure 6 decrease fast for the first variation after then it decreases slowly on increases of $Sc$. On increase in time $t$, boundary layer thickness of velocity increases in figure 20, thickness of thermal boundary layer in figure 21 and concentration boundary layer in figure 22 are approximately same.

Table 1 represents the values of the skin friction coefficient, Nusslet number, and Sherwood number for different values of physical parameters. Table reveals that Skin friction is higher for increase $Du$, $M$, $So$, $R$, $t$ and lower for $Sc$, $Kr$, $Pr$. Nusselt number is lower for increment of $Du$, $Sc$, $Kr$, $M$, $R$, $t$ and higher for increment of $Pr$, $So$. Sherwood number increases for increase $Du$, $Sc$, $Kr$, $M$, $M$, $R$ and Sherwood number decreases for increase $Pr$, $So$, $t$.

## 5. Conclusion

The following findings have been drawn for this model based on the investigation of unsteady MHD flow across a vertical porous plate under variable suction velocity with Soret-Dufour, second-order chemical reaction, variable temperature, and variable concentration:

(1).As the radiation parameter increases, the velocity increases slowly close to the plate before increasing quickly.

(2).There is an appealing impact of concentration on the Schmidt number change.

(3). Velocity increases and exhibits a positive change in the vicinity of the plate as the Soret number rises.

(4).As the Dufour number rises, a decrease in concentration is seen close to the plate, while an increase in velocity is observed at a distance.
(5).Velocity drops, temperature gradually changes, and concentration drops close to the plate as the rate of reaction parameter increases.


## Acknowledgement

We comply with the help of our principal of our college Dr. V. C. Tripathi and proctor of science faculty of our college Dr. A. K. Dwivedi and thank you for encouraging us to complete this project.

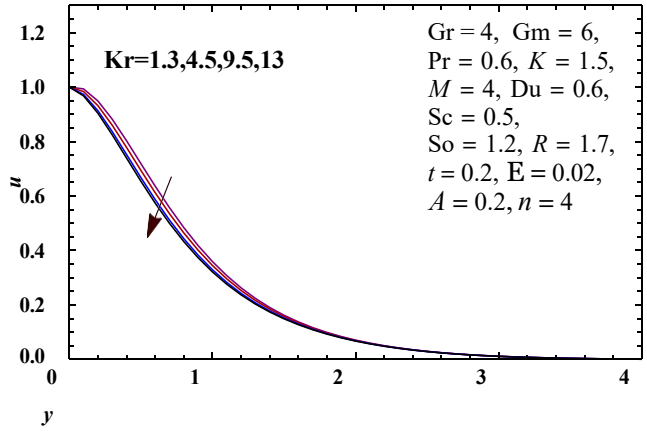




**Figure 1.** **Velocity Profiles for Different Values of** *Kr*

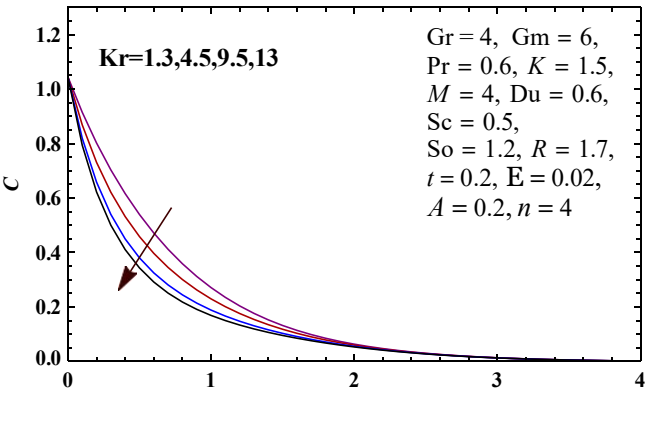



Figure 2. Concentration Profiles for Different Values of *Kr*

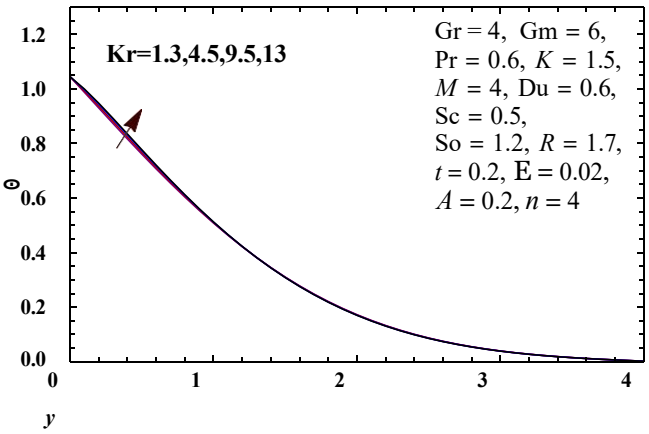



Figure 3. Temperature Profiles for Different Values of *Kr*

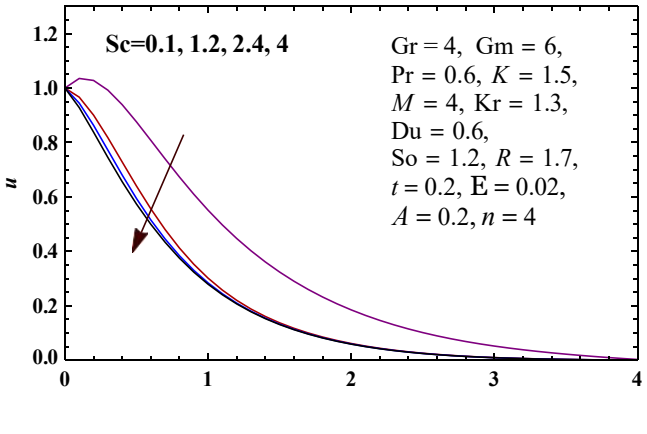



**Figure 4.** **Velocity Profiles for Different Values of** *Sc*

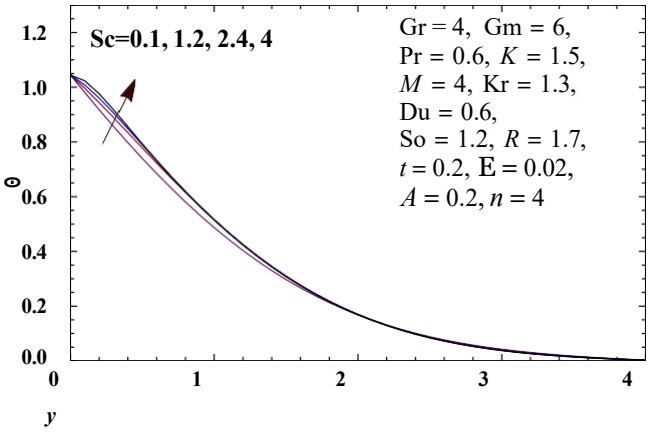



**Figure 5.** **Temperature Profiles for Different Values of** *Sc*

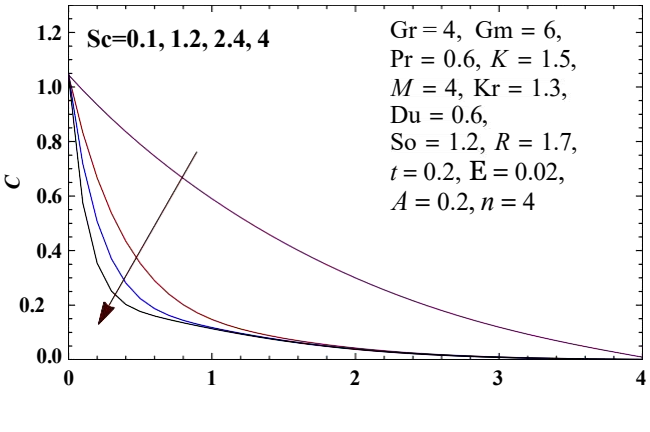



Figure 6. Concentration Profiles for Different Values of *Sc*

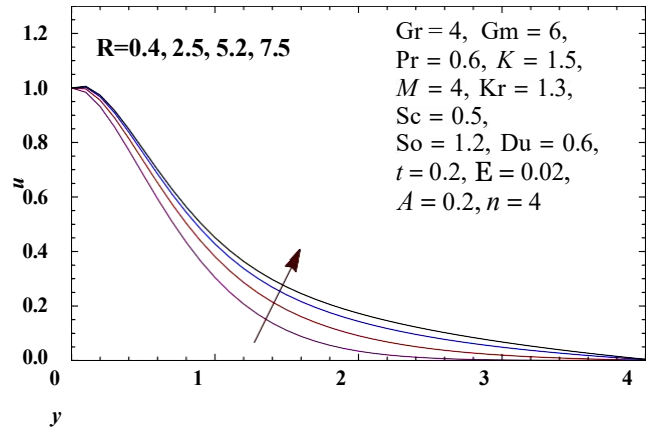



**Figure 7.** **Velocity Profiles for Different Values of** *R*

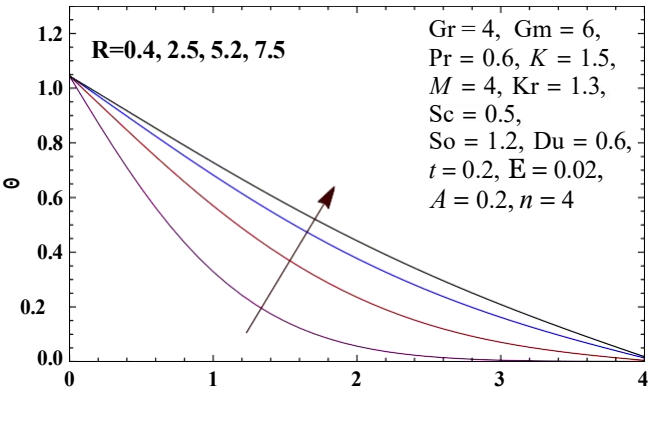



**Figure 8.** **Temperature Profiles for Different Values of** *R*

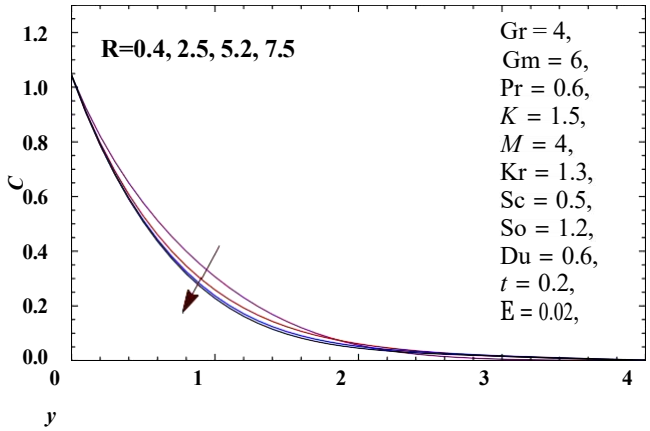



Figure 9. Concentration Profiles for Different Values of *R*

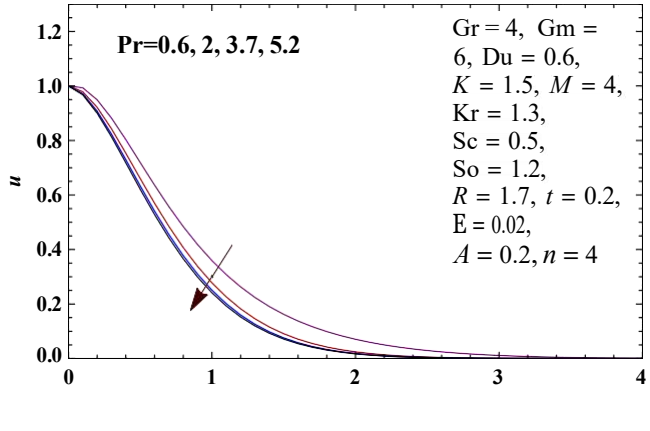



**Figure 10.** **Velocity Profiles for Different Values of** *Pr*

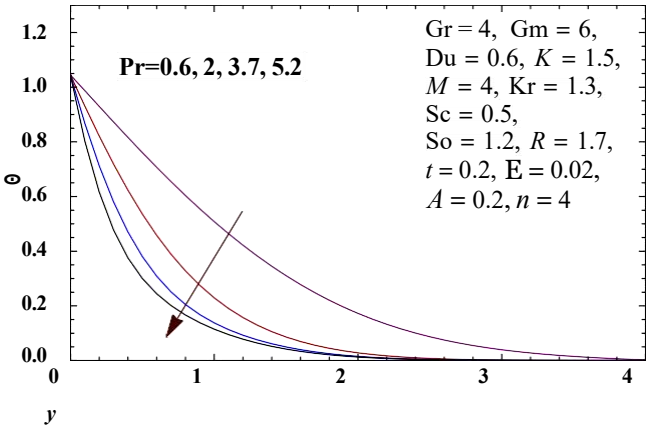



Figure 11. Temperature Profiles for Different Values of *Pr*

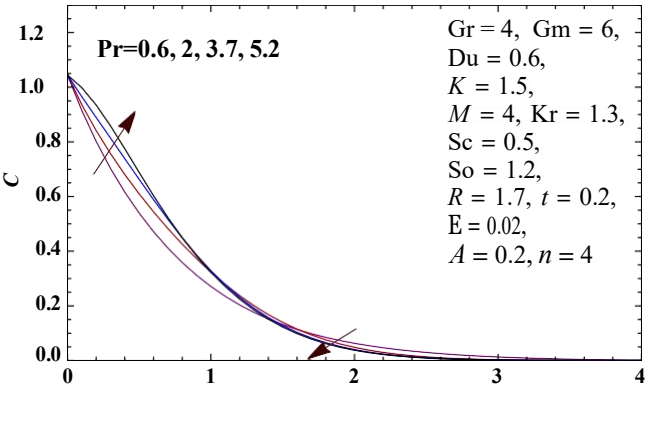



**Figure 12. Velocity Profiles for Different Values of *Pr***

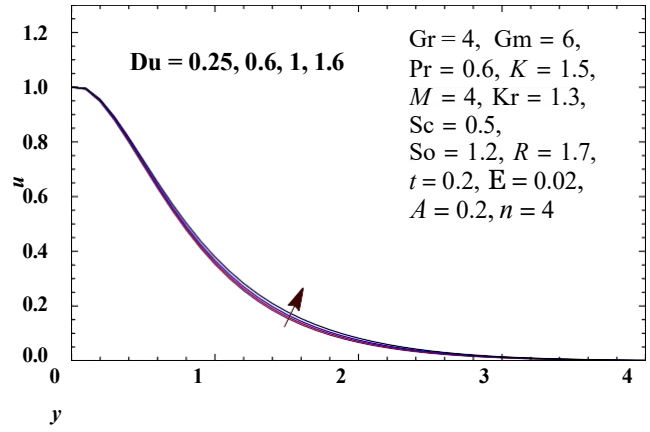



**Figure 13. Velocity Profiles for Different Values of *Du***

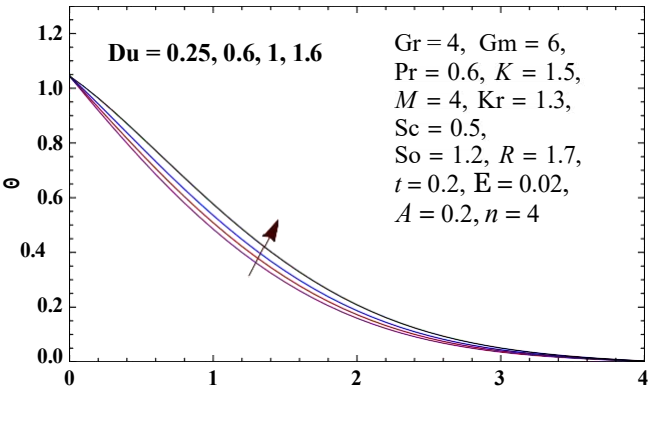



Figure 14. Temperature Profiles for Different Values of *Du*

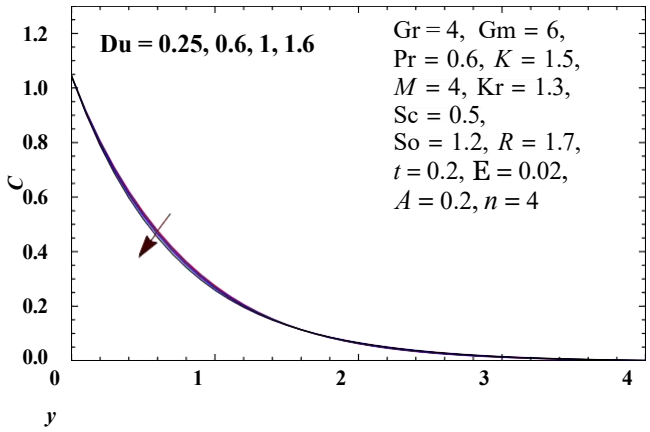



Figure 15. Concentration Profiles for Different Values of *Du*

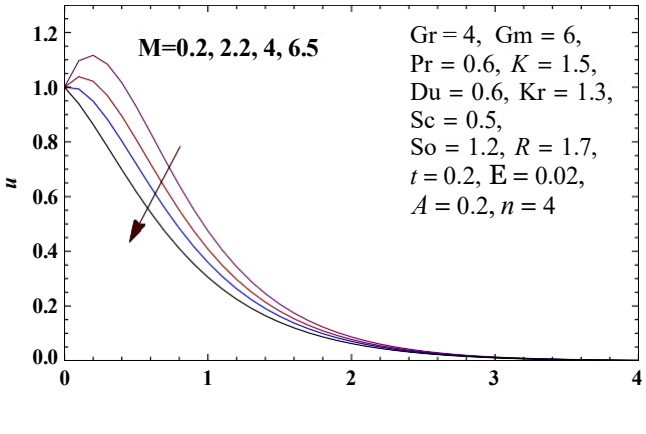



**Figure 16. Velocity Profiles for Different Values of *M***

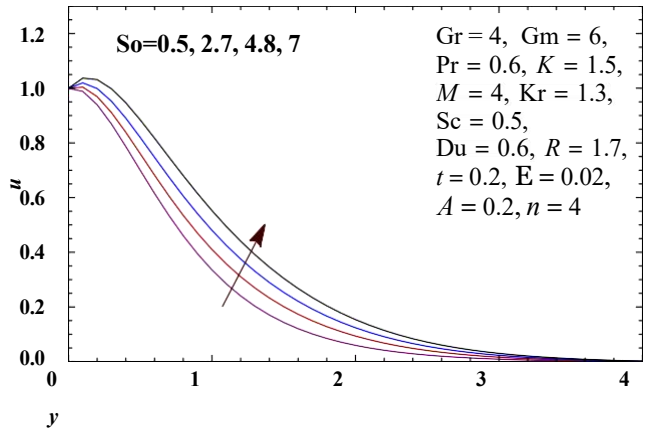



**Figure 17.** **Velocity Profiles for Different Values of** *Sr*

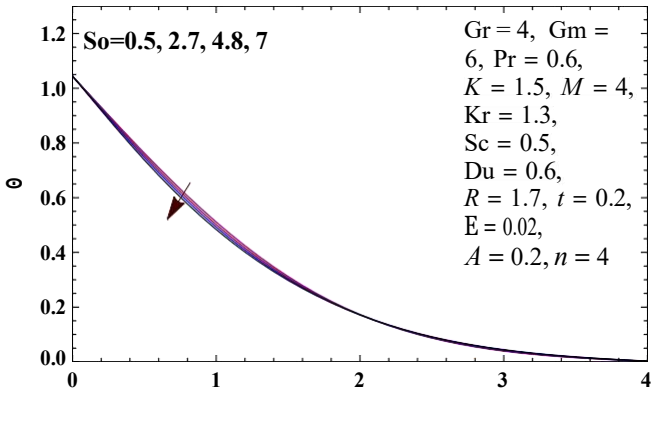



Figure 18. Temperature Profiles for Different Values of *Sr*

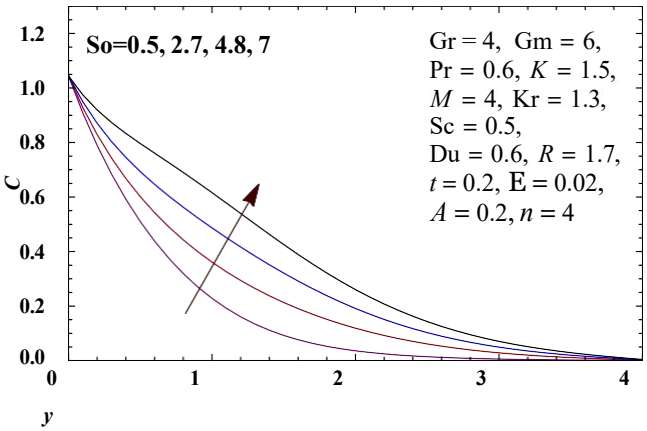



Figure 19. Concentration Profiles for Different Values of *Sr*

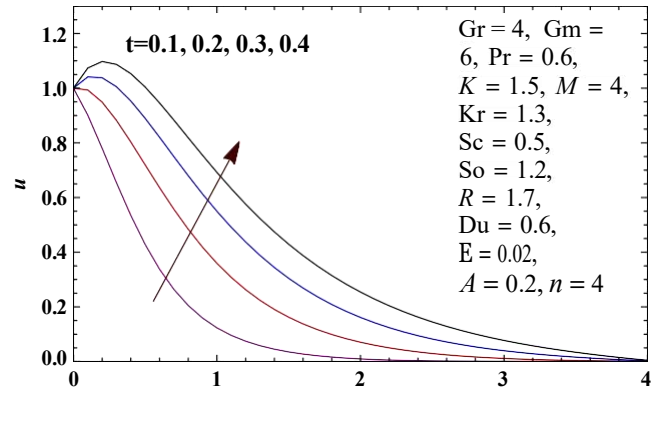



**Figure 20.** **Velocity Profiles for Different Values of** *t*

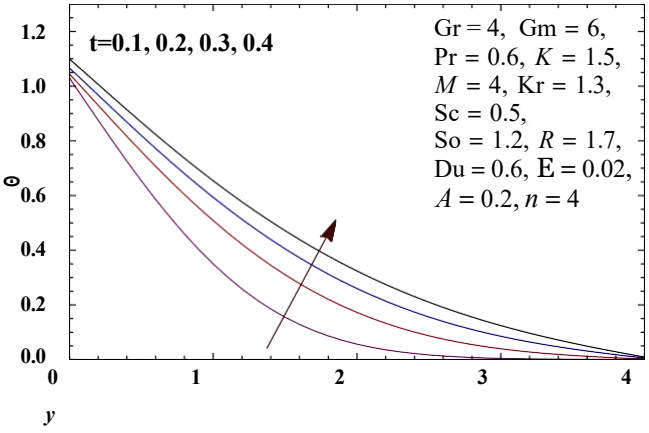



**Figure 21.** **Temperature Profiles for Different Values of** *t*

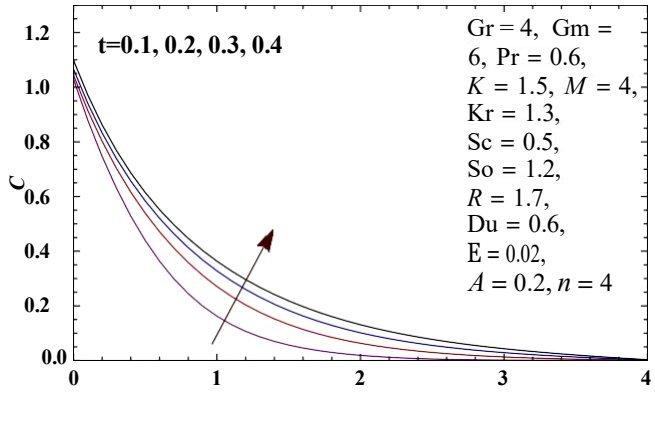



Figure 22. Concentration Profiles for Different Values of *t*

| $Du$ | $Kr$ | $M$ | $Pr$ | $So$ | $Sc$ | $R$ | $t$ | $\tau$ | $Nu$ | $Sh$ |
|---|---|---|---|---|---|---|---|---|---|---|
| 0.25 | 1.3 | 4 | 0.6 | 1.2 | 0.5 | 1.7 | 0.2 | −0.0806652 | 0.631965 | 1.2725 |
| 0.6 | 1.3 | 4 | 0.6 | 1.2 | 0.5 | 1.7 | 0.2 | −0.0680455 | 0.57171 | 1.29659 |
| 1 | 1.3 | 4 | 0.6 | 1.2 | 0.5 | 1.7 | 0.2 | −0.0532918 | 0.498964 | 1.32602 |
| 1.6 | 1.3 | 4 | 0.6 | 1.2 | 0.5 | 1.7 | 0.2 | −0.0304486 | 0.381013 | 1.37455 |
| 0.6 | 1.3 | 4 | 0.6 | 1.2 | 0.5 | 1.7 | 0.2 | −0.0680455 | 0.57171 | 1.29659 |
| 0.6 | 4.5 | 4 | 0.6 | 1.2 | 0.5 | 1.7 | 0.2 | −0.165811 | 0.525655 | 1.75917 |
| 0.6 | 9.5 | 4 | 0.6 | 1.2 | 0.5 | 1.7 | 0.2 | −0.270591 | 0.47564 | 2.2504 |
| 0.6 | 13 | 4 | 0.6 | 1.2 | 0.5 | 1.7 | 0.2 | −0.324344 | 0.449315 | 2.50522 |
| 0.6 | 1.3 | 0.2 | 0.6 | 1.2 | 0.5 | 1.7 | 0.2 | −0.0806652 | 0.631965 | 1.2725 |
| 0.6 | 1.3 | 2.2 | 0.6 | 1.2 | 0.5 | 1.7 | 0.2 | 0.383285 | 0.57171 | 1.29659 |
| 0.6 | 1.3 | 4 | 0.6 | 1.2 | 0.5 | 1.7 | 0.2 | −0.0680455 | 0.57171 | 1.29659 |
| 0.6 | 1.3 | 6.5 | 0.6 | 1.2 | 0.5 | 1.7 | 0.2 | −0.605199 | 0.57171 | 1.29659 |
| 0.6 | 1.3 | 4 | 0.6 | 1.2 | 0.5 | 1.7 | 0.2 | −0.0680455 | 0.57171 | 1.29659 |
| 0.6 | 1.3 | 4 | 2 | 1.2 | 0.5 | 1.7 | 0.2 | −0.212385 | 1.13422 | 1.08335 |
| 0.6 | 1.3 | 4 | 3.7 | 1.2 | 0.5 | 1.7 | 0.2 | −0.286346 | 1.76295 | 0.791948 |
| 0.6 | 1.3 | 4 | 5.2 | 1.2 | 0.5 | 1.7 | 0.2 | −0.326854 | 2.21339 | 0.462493 |
| 0.6 | 1.3 | 4 | 0.6 | 0.5 | 0.5 | 1.7 | 0.2 | −0.116983 | 0.56595 | 1.35887 |
| 0.6 | 1.3 | 4 | 0.6 | 2.7 | 0.5 | 1.7 | 0.2 | −0.0390785 | 0.58478 | 1.15756 |
| 0.6 | 1.3 | 4 | 0.6 | 4.8 | 0.5 | 1.7 | 0.2 | 0.195199 | 0.605142 | 0.946436 |
| 0.6 | 1.3 | 4 | 0.6 | 7 | 0.5 | 1.7 | 0.2 | 0.36856 | 0.630033 | 0.69558 |
| 0.6 | 1.3 | 4 | 0.6 | 1.2 | 0.1 | 1.7 | 0.2 | 0.351464 | 0.641045 | 0.563936 |
| 0.6 | 1.3 | 4 | 0.6 | 1.2 | 1.2 | 1.7 | 0.2 | −0.335173 | 0.487006 | 2.11836 |
| 0.6 | 1.3 | 4 | 0.6 | 1.2 | 2.4 | 1.7 | 0.2 | −0.554599 | 0.365919 | 3.26151 |
| 0.6 | 1.3 | 4 | 0.6 | 1.2 | 4 | 1.7 | 0.2 | −0.718693 | 0.212302 | 4.69537 |
| 0.6 | 1.3 | 4 | 0.6 | 1.2 | 0.5 | 0.4 | 0.2 | −0.158118 | 0.464883 | 1.19349 |
| 0.6 | 1.3 | 4 | 0.6 | 1.2 | 0.5 | 2.5 | 0.2 | −0.0357433 | 0.493682 | 1.32001 |
| 0.6 | 1.3 | 4 | 0.6 | 1.2 | 0.5 | 5.2 | 0.2 | 0.0291802 | 0.364647 | 1.35436 |
| 0.6 | 1.3 | 4 | 0.6 | 1.2 | 0.5 | 7.5 | 0.2 | 0.0607162 | 0.315013 | 1.36687 |
| 0.6 | 1.3 | 4 | 0.6 | 1.2 | 0.5 | 1.7 | 0.1 | −0.987251 | 0.773219 | 1.50378 |
| 0.6 | 1.3 | 4 | 0.6 | 1.2 | 0.5 | 1.7 | 0.2 | −0.0680455 | 0.57171 | 1.29659 |
| 0.6 | 1.3 | 4 | 0.6 | 1.2 | 0.5 | 1.7 | 0.3 | 0.412517 | 0.493131 | 1.25483 |
| 0.6 | 1.3 | 4 | 0.6 | 1.2 | 0.5 | 1.7 | 0.4 | 0.737488 | 0.461259 | 1.27625 |

Table 1. Skin friction coefficient $\tau$, Nusselt number $Nu$ and Sherwood number $Sh$ for different values of parameters taking fix values of $\epsilon = 0.02$, $A = 0.2$, $n = 4$, $K = 1.5$, $Gr = 4$, $Gm = 6$

## References


[1] M. J. Babu and N. Sandeep, *Effect of nonlinear thermal radiation on non-aligned bio-convective stagnation point flow of a magnetic-nanofluid over a stretching sheet*, Alexandria Engineering Journal, 55(3)(2016), 1931-1939.

[2] K. Rushi, S. Palani and P. K. Kameswaran, *Unsteady MHD flow over a stretching surface with higher order chemical reaction*, Ain Shams Engineering Journal, 7(1)(2016), 399-408.

[3] A. Mastroberardino, M. Madsen, J. Hirschhorn and J. I. Siddique, *Magnetohydrodynamic boundary layer slip flow and heat transfer of power-law fluid over a flat plate*, Journal of Applied Fluid Mechanics, 9(1)(2016), 11-17.

[4] A. S. Idowu and B. O. Falodun, *SoretDufour effects on MHD heat and mass transfer of Walters-B viscoelastic fluid over a semi-infinite vertical plate: spectral relaxation analysis*, Journal of taibah university for science, 13(1)(2019), 4962.

[5] K. Saritha, M. N. Rajasekhar and B. S. Reddy, *Combined effects of Soret and Dufour on MHD flow of a power-law fluid over flat plate in slip flow regime*, Int. J. of Applied Mechanics and Engineering, 23(3)(2018), 689-705.

[6] M. Y. Malik and Khalil-ur-Rehman, *Effects of Second Order Chemical Reaction on MHD Free Convection*

*Dissipative Fluid Flow past an Inclined Porous Surface by way of Heat Generation: A Lie Group Analysis*, Inf. Sci. Lett., 5(2)(2016), 35-45.

[7] M. Imtiaz, H. Nazar and T. Hayat, *Soret and Dufour effects in the flow of viscous fluid by a curved stretching surface*, Pramana - J. Phys., 94(2020), Article number 48.

[8] S. Anuradha and N. Harianand, *A study of Dufour and Soret effect on MHD mixed convection stagnation point flow towards a vertical plate in a porous medium*, International Journal of Fluids Engineering, 9(1)(2017), 1-8.

[9] Brice Carnahan, H. A. Luther and James O. Wilkes, *Applied Numerical Methods*, Krieger Pub Co, Florida, (1990).

[10] N. Ahmed, *Heat and mass transfer in MHd Poiseuille flow with porous walls*, Journal of Engineering Physics and Thermophysics, 92(1)(2019), 128-136.

[11] U. J.Das, and S. Dorje, *Magnetohydrodynamic boundary layer flow with Soret/Dufour effects in presence of heat source and chemical reaction*, International Journal of Applied Engineering Research, 14(2)(2019), 485-490.

[12] R. Siegel and J. R. Howell, *Thermal Radiation Heat Transfer*, Taylor & Francis, London, (1992).